Supporting Information for "A Study on Inferring Daytime Variations of XCO_2 from Current and Future Space-Based Missions"

Calla Marchetti[1,2,*], Jonathan Hobbs[1], Peter Somkuti[3,4], Joshua Laughner[1]

[1]Jet Propulsion Laboratory, California Institute of Technology, Pasadena, CA, USA

[2]Department of Atmospheric and Oceanic Sciences, University of California Los Angeles, Los Angeles, CA, USA

[3]Earth System Science Interdisciplinary Center, University of Maryland, College Park, MD, USA

[4]Global Modeling and Assimilation Office, National Aeronautics and Space Administration, Goddard Space Flight Center, Greenbelt, MD, USA

[*]now at: Department of Atmospheric and Oceanic Sciences, Princeton University, Princeton, NJ, USA

Contents of this file

Introduction In this supplement we show model performance statistics for individual TCCON sites, as opposed to the combined statistics in the main text. For each simulation ran, we give the R^2 and RMSE values for each TCCON site for both diurnal cycle comparison and drawdown comparison. We also detail our recursive feature elimination process, and show expanded figures with more examples than the ones in the main text. Additionally, we describe how a simplification made in our matching of OCO-3 and OCO-3 data does not affect the conclusions of the paper.

S1: Recursive Feature Elimination For our recursive feature elimination we run the model repetitively, with each run having one less feature in the feature set than the previous run. We run the model three times per feature set, and after each run we record the model outputted permutation importance, which assigns a value to each feature. At the end of the three runs we average the importance values across the runs, and remove the feature with the least importance. We continue this process until all the features have been removed in order of importance, with the final run being a model trained only on the most important feature. This process allows us to see how model performance improves as we add features in, and also allows us to look for possible redundancies in our feature set, such as from instances where features are commonly grouped together in order of importance but performance doesn't change by the removal or addition of one. We run an RFE for both the OCO-2/3 crossing simulation and the 3 point ideal drawdown simulation. For the 3 point ideal drawdown simulation we removed the difference in XCO_2 feature, denoted "diff_XCO_2" because when the points are a fixed distance apart the way they are in the 3 point simulation, "diff_XCO_2" is a scale multiple of the time derivative "delta_XCO_2".

S2: Impact of incorrectly summarizing OCO-2/3 crossings with multiple OCO-3 orbits In the main paper, we described our algorithm for identifying cases where OCO-2 and OCO-3 cross, i.e., observe the same location. In order to minimize the size of the netCDF files storing these crossings, the files were designed to store the IDs of the first and last soundings for both OCO-2 and OCO-3 that are contained in one crossing. In cases where multiple OCO-3 orbits pass within the same set of OCO-2 soundings, this means that simply taking all OCO-3 soundings between the given sounding IDs will incorrectly include many soundings far away from the OCO-2 soundings (Fig. S4).

Our analysis to determine the probability distributions for the OCO-2/OCO-3 crossing simulation did incorrectly include these intervening OCO-3 soundings. Fortunately, cases with multiple OCO-3 orbits matching with one OCO-2 orbit are in the minority (1770 multiple orbit crossings vs. 22,218 single orbit crossings in our sampled years), so this should not significantly alter the distribution of OCO-3 times relative to OCO-2. To confirm, Fig. S10 shows histograms of the OCO-3 time relative to OCO-2 for both just the crossings with a single OCO-3 orbit and all crossings, including the intervening soundings incorrectly included in the multi-orbit crossings. The distributions are very similar; therefore, we retained our existing OCO-2/3 crossing simulations performed with probability distributions derived from the latter histogram.

The crossing widths plotted in Fig. S5 do not include the erroneous intervening OCO-3 soundings. To remove those erroneous soundings, we first split the range of soundings identified by the initial crossing algorithm by finding time gaps greater than 0.77 h (approximately one-half of an ISS orbit). Then, within each orbit, we calculated the shortest great circle distance between each OCO-3 sounding and any of the OCO-2 soundings and removed the OCO-3 sounding if that distance exceeded 100 km. Note that Fig. S5 includes all crossings in years 2020 to 2022, not just those near TCCON sites.

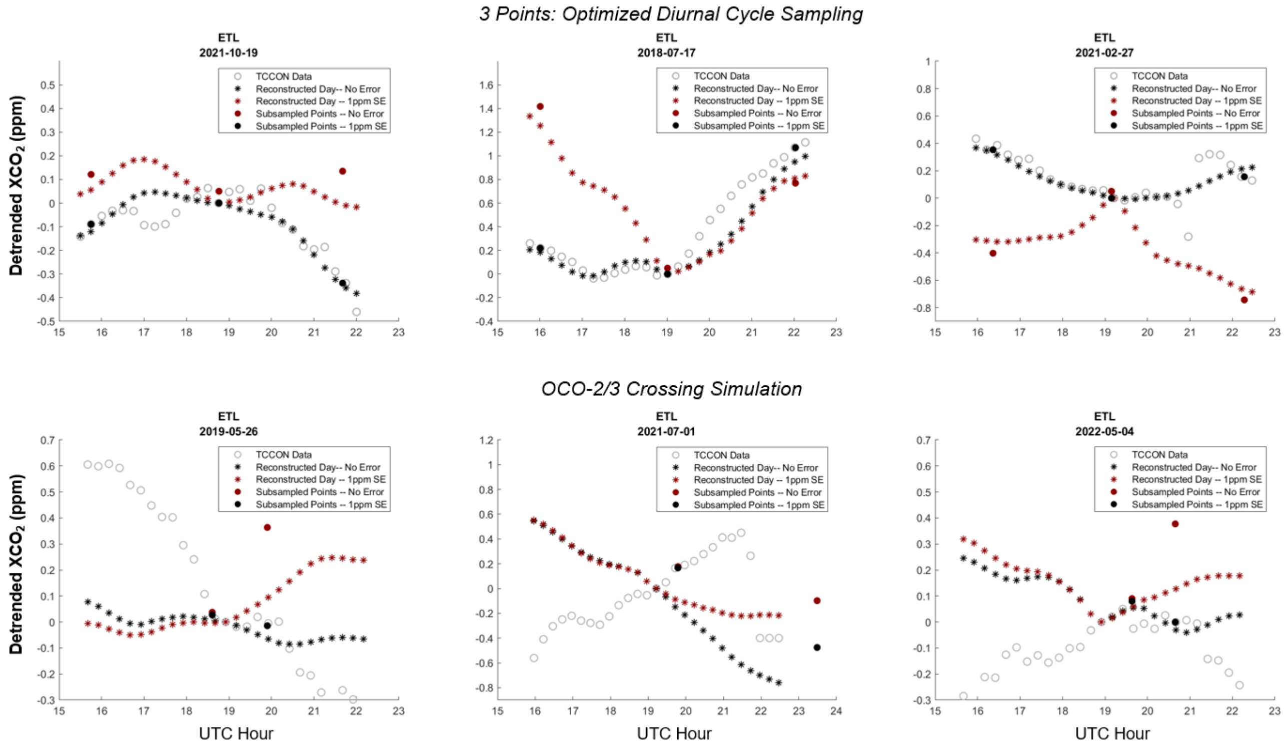

Figure S1. Examples of how error affects model predicted diurnal cycles for two different simulations: the 3 point ideal diurnal cycle sampling times (-3, 0, +3 hr) and the OCO-2/3 crossing sampling pattern. The grey hollow circles show the true diurnal cycle, as taken from the TCCON data. The filled circles show the diurnal cycles predicted by the model (with and without error) and the "subsampled points" are the points used to calculate the ΔXCO_2 the model received as input (with and without error added). For each sampling pattern we had the model predict the day where XCO_2 has a standard error of 0ppm, and then with a standard error of 1ppm.

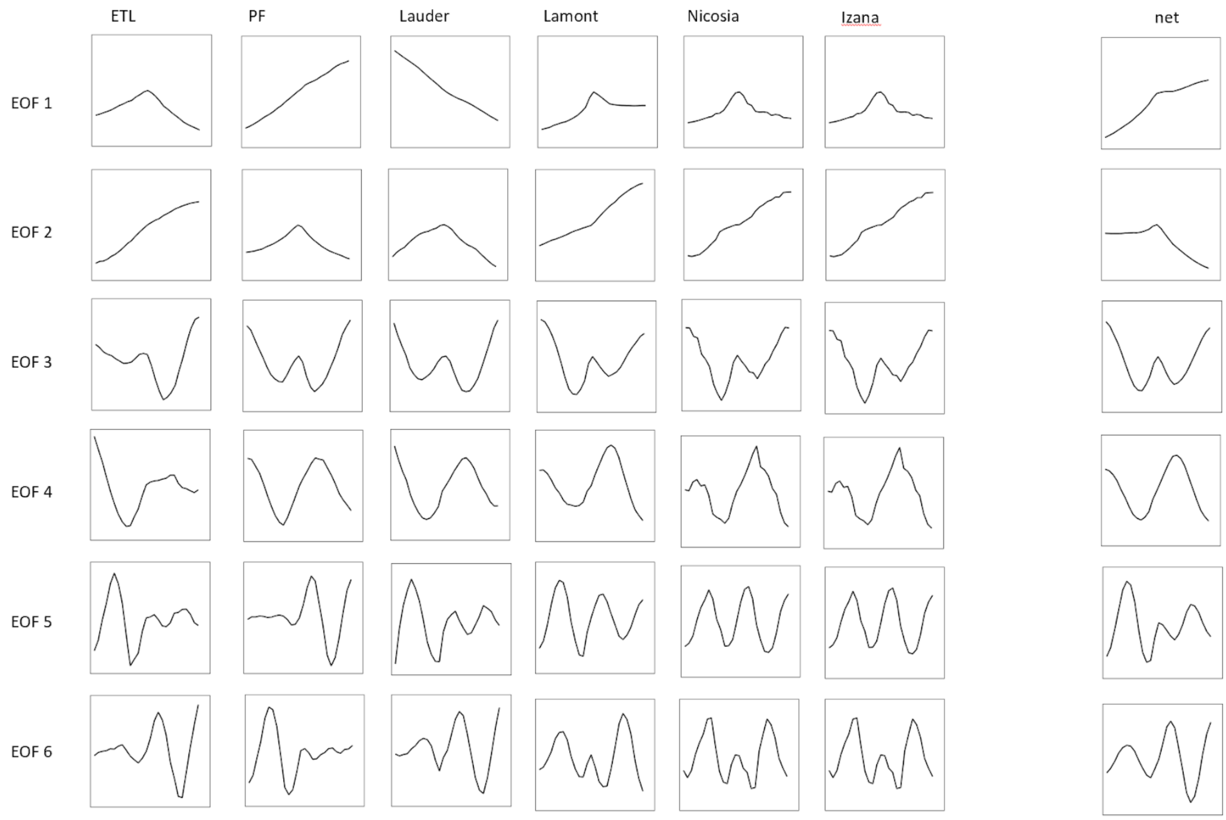

Figure S2. EOFs calculated from individual TCCON sites' data (one site per column) and the EOFs from all six sites combined ("net").

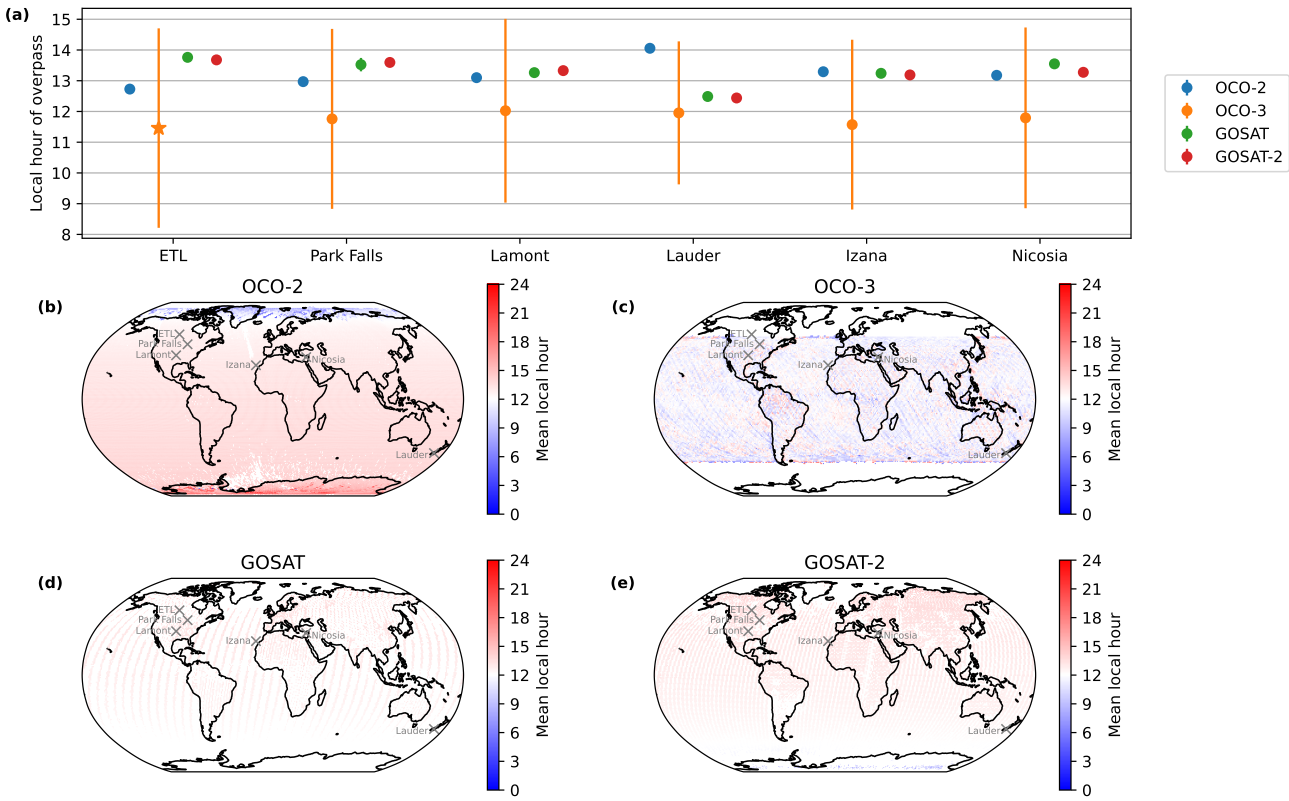

Figure S3. Local overpass times for OCO-2, OCO-3, GOSAT, and GOSAT-2 calculated for the year 2021. Local times are calculated by adding a number of hours equal to the longitude of each sounding divided by 15°. **(a)** The mean and standard deviation of the local times for each satellite in a 5° longitude by 4° latitude box containing each TCCON site (given as the x-axis label); OCO-3 for ETL uses a star to indicate that a box south of ETL's actual location was used, since OCO-3's maximum latitude is south of ETL's actual location. **(b)** through **(d)** show maps of the mean local time for each satellite in $1° \times 1°$ grid boxes.

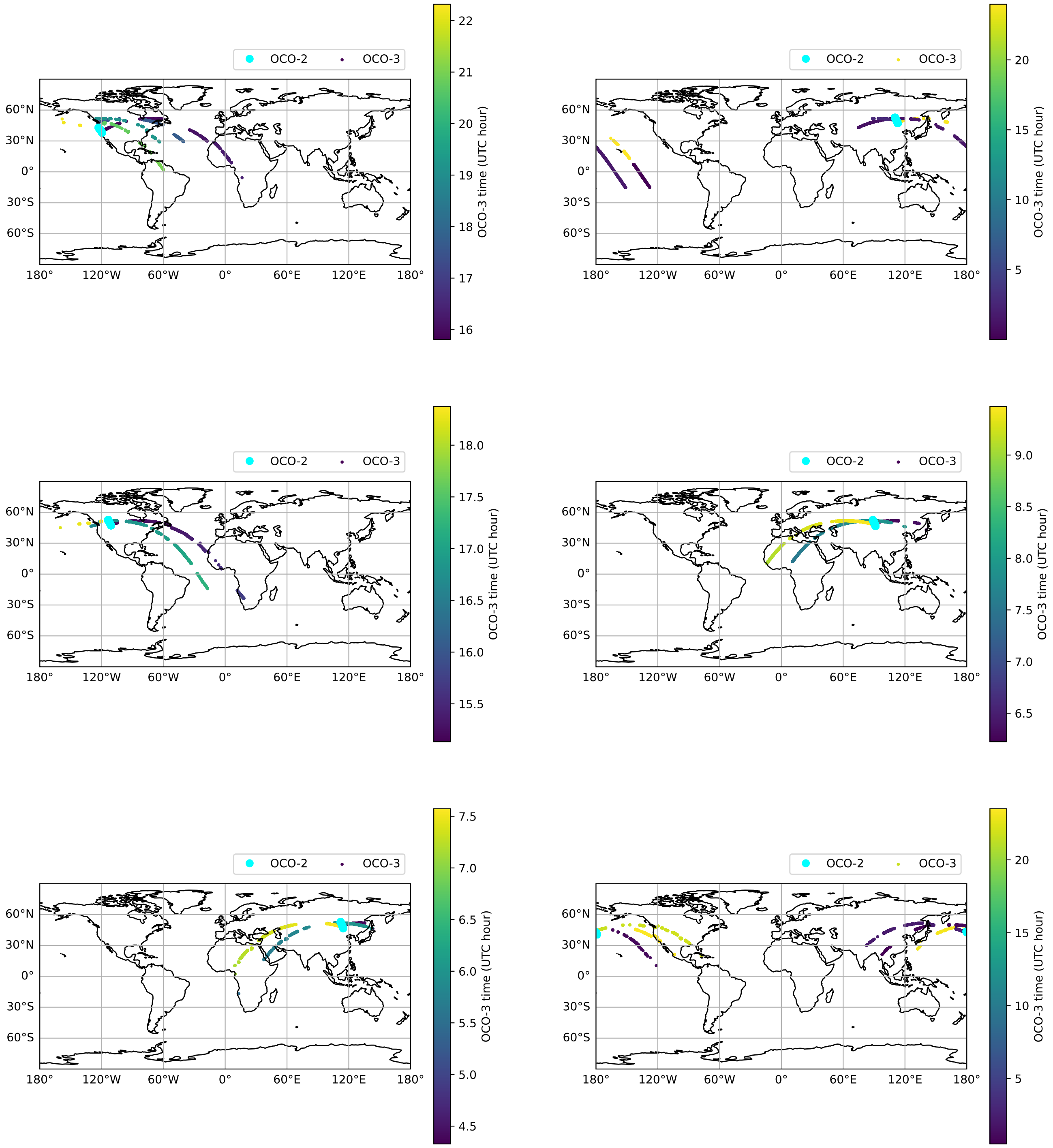

Figure S4. Examples of 6 OCO-2/OCO-3 crossings where multiple OCO-3 orbits matched with a given set of OCO-2 soundings. The cyan markers show the OCO-2 soundings, and the smaller markers show the OCO-3 soundings (colored by their UTC time). All OCO-3 soundings between the first and last ones matched with OCO-2 soundings are show to illustrate the problem caused by summarizing the crossings with the first and last soundings to include.

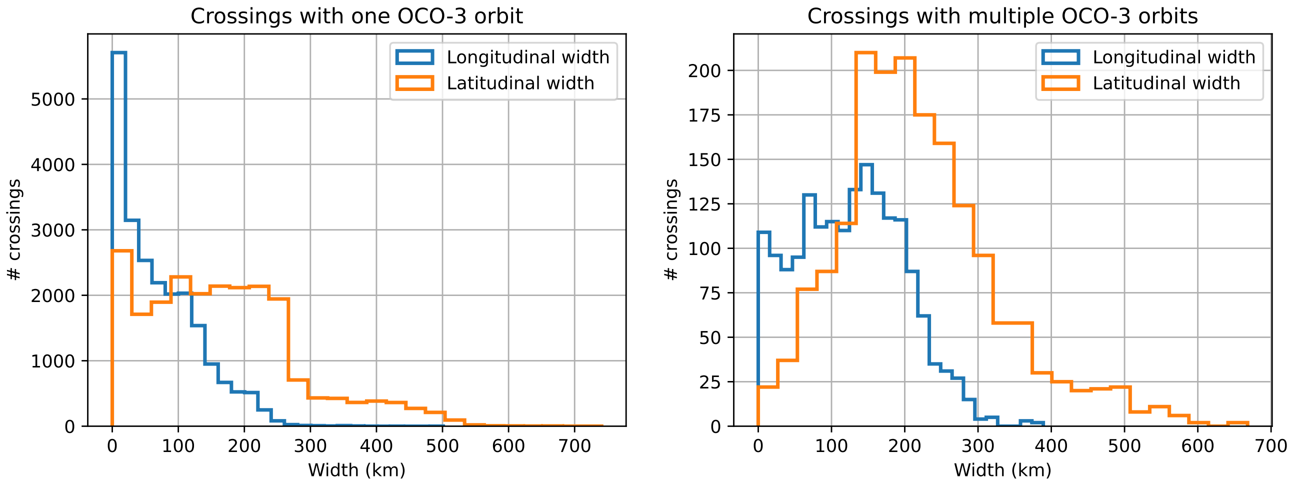

Figure S5. Widths of all individual OCO-2/OCO-3 crossings along their north-south (latitudinal) and east-west (longitudinal) directions for years 2020 to 2022. These widths are calculated as the great circle distance between the minimum and maximum longitude and latitude of all the OCO-2 and -3 soundings included in the crossing. For the longitudinal distance, the latitude is set to halfway between the minimum and maximum latitude, since latitude affects the distance between two given longitudes. The left panel is for crossings that matched only a single OCO-3 orbit to OCO-2 and the right panel shows crossings with multiple OCO-3 orbits. In the latter, the OCO-3 soundings were restricted to those within 100 km of any OCO-2 sounding.

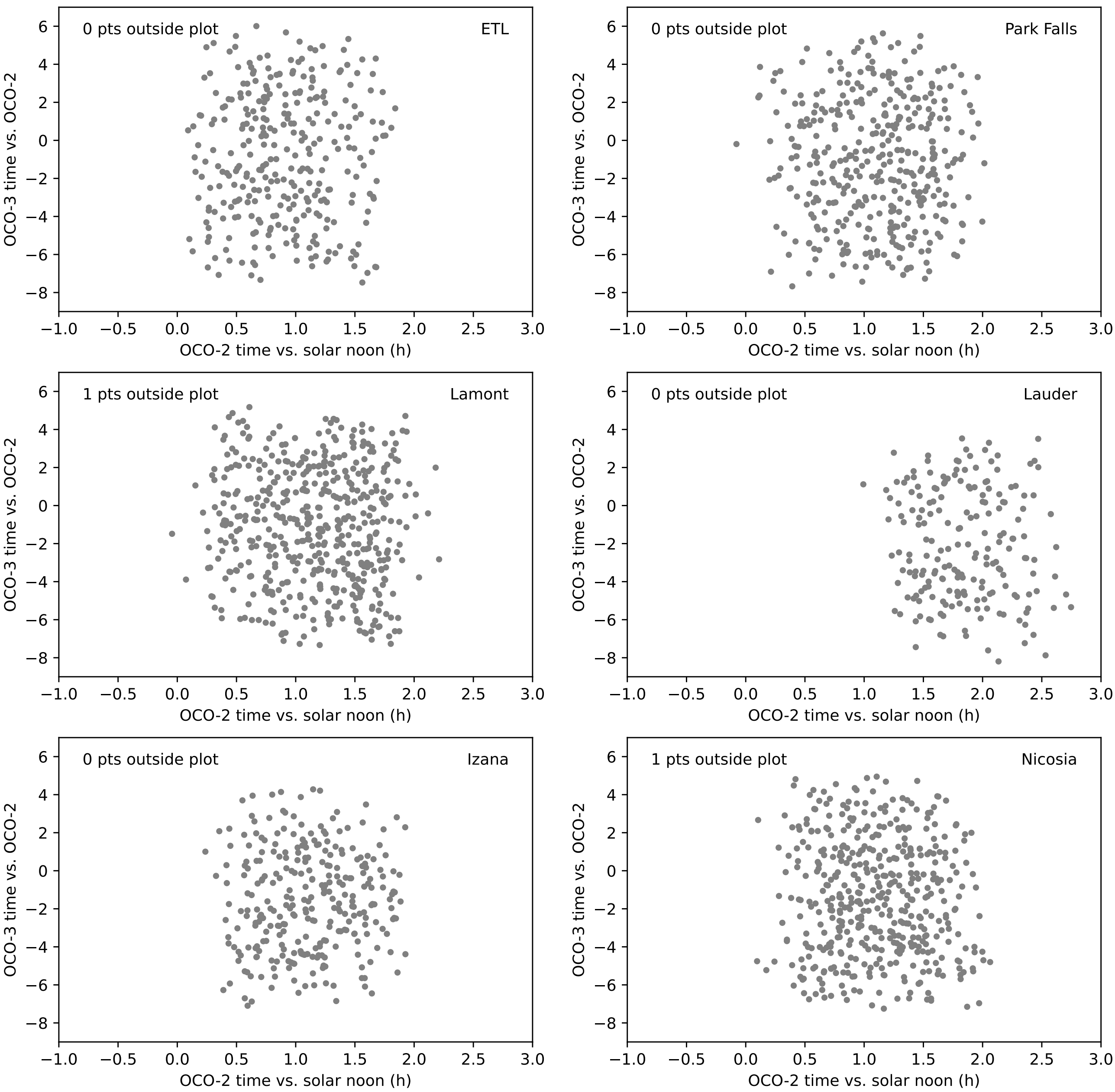

Figure S6. Relationship between OCO-2 time relative to solar noon and OCO-3 time relative to OCO-2 for each of the six TCCON sites used in our analysis. No correlations is observed between these variables.

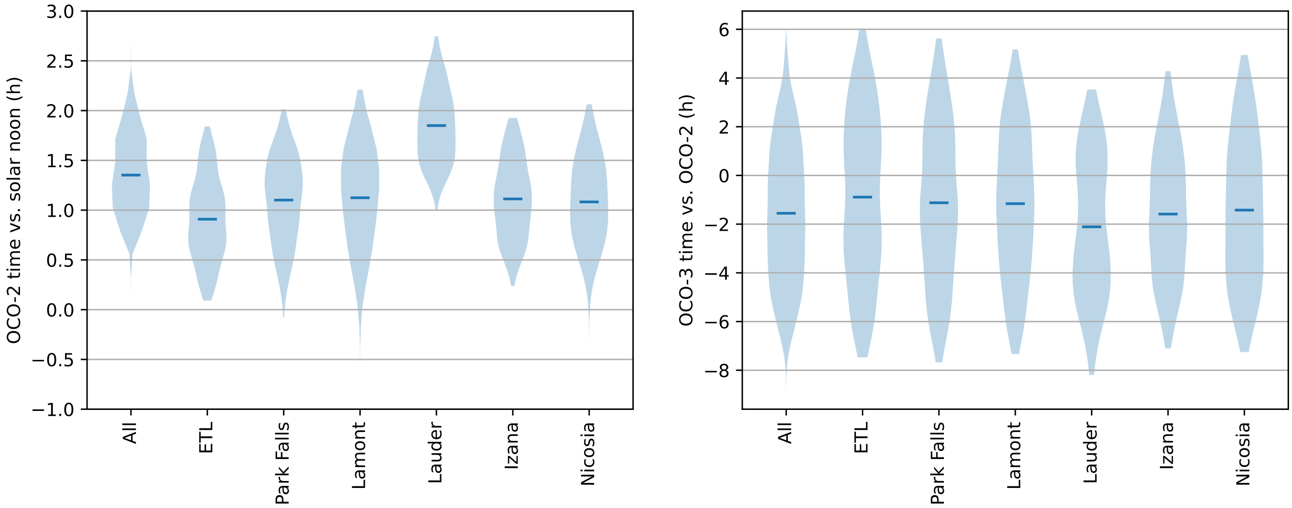

Figure S7. Violin plots of the distribution of mean OCO-2 time relative to solar noon (left panel) and mean OCO-3 time relative to OCO-3 (right panel) for all OCO-2/OCO-3 crossings with a single OCO-3 orbit. The horizontal lines indicate the mean of each distribution.

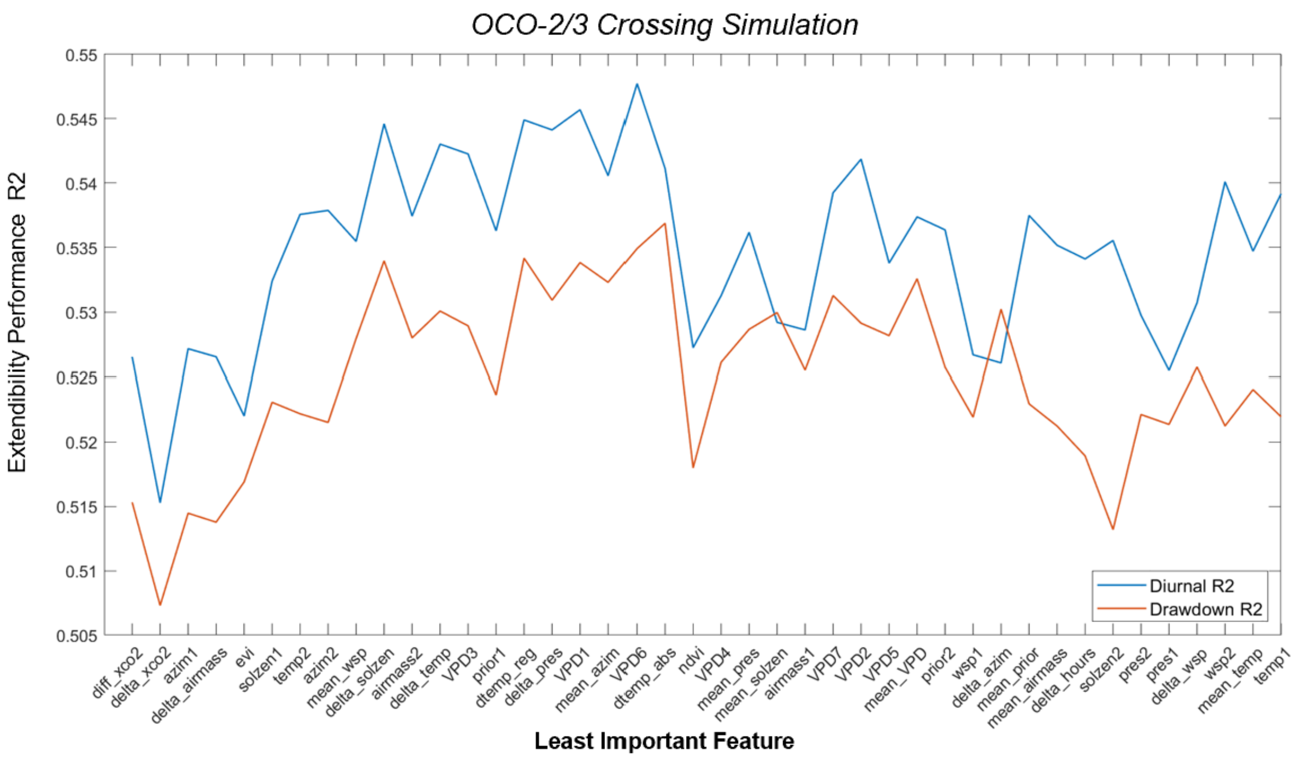

Figure S8. Recursive feature elimination for the OCO-2/3 crossing simulation with NDVI and EVI included.

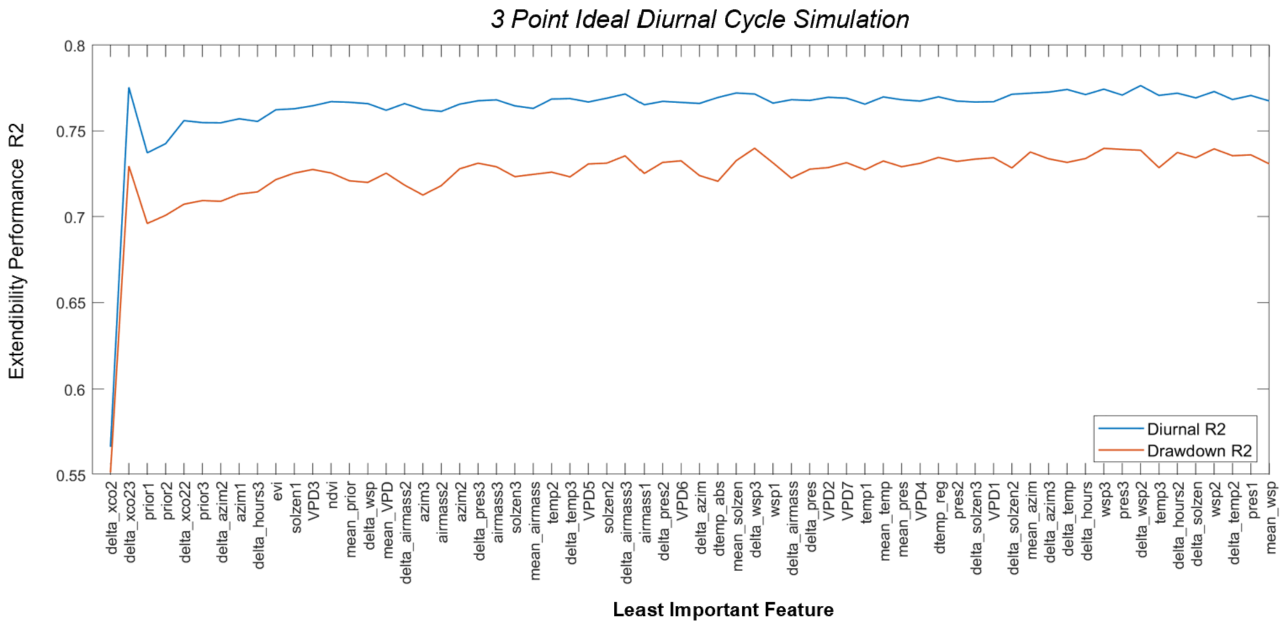

Figure S9. Recursive feature elimination for the simulation with 3 observations 3 hours apart with NDVI and EVI included.

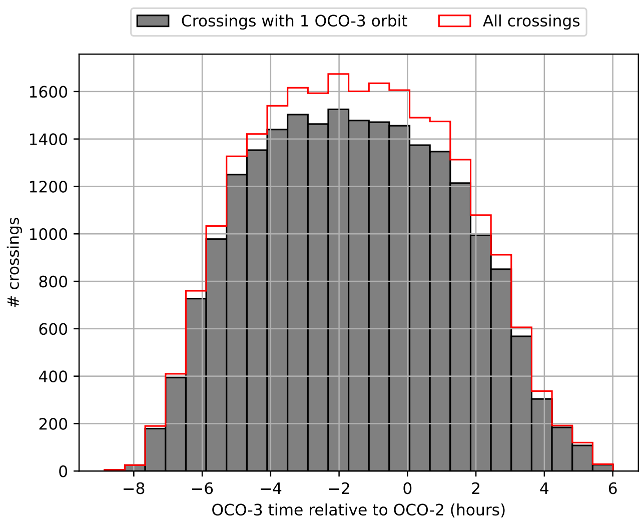

Figure S10. Histogram of the mean OCO-3 overpass time relative to OCO-2. The gray bars show the distribution for cases where only one OCO-3 orbit matched with OCO-2; the red line shows the distribution for all crossings, including cases with more than 1 OCO-3 orbit. In those cases, the mean time is the mean of all soundings between the first and last OCO-3 sounding to match with OCO-2, not just those within a given distance of the OCO-2 soundings.

Table S1. Model Performance (R^2) for the OCO-2/3 crossing simulation. Each site listed describes the model run where that TCCON site is left out of EOF generation and the train/test split and used as the extendibility test site. The "Train" column shows model performance on data it was trained on and the "Test" column shows model performance on data it has not seen before. "Extendility" columns show model performance on the TCCON site that was withheld from EOF generation and model training, with the "Opt." version being the optimistic scenario where systematic error cancels out when adding simulated uncertainty, and the "Pess" version being the pessimistic scenario where systematic error does not cancel out when adding simulated uncertainty. The "PTP" sub-column describes the diurnal cycle comparison performance, and the "Draw" sub-column describes the drawdown performance.

Site	Training		Testing		Opt. Extendibility		Pess. Extendibility	
	PTP	Draw.	PTP	Draw.	PTP	Draw.	PTP	Draw.
ETL	0.85	0.84	0.55	0.54	0.53	0.56	0.43	0.40
PF	0.85	0.84	0.54	0.51	0.54	0.54	0.43	0.42
Lauder	0.85	0.84	0.54	0.56	0.52	0.49	0.50	0.40
Lamont	0.84	0.83	0.56	0.57	0.52	0.51	0.47	0.45

Table S2. Model Performance (RMSE) for the OCO-2/3 crossing simulation. The column descriptions follow Table S1.

Site	Training		Testing		Opt. Extendibility		Pess. Extendibility	
	PTP	Draw.	PTP	Draw	PTP	Draw	PTP	Draw
ETL	0.12	0.16	0.26	0.35	0.25	0.35	0.30	0.50
PF	0.12	0.16	0.25	0.33	0.30	0.41	0.36	0.54
Lauder	0.13	0.18	0.28	0.36	0.19	0.27	0.23	0.33
Lamont	0.11	0.16	0.24	0.34	0.30	0.32	0.32	0.50

Table S3. Model Performance (R^2) for the OCO-3 self crossing simulation. ETL and PF are the only sites shown due to the locations of OCO-3 self crossings.The column descriptions follow Table S1.

Site	Training		Testing		Opt. Extendibility		Pess. Extendibility	
	PTP	Draw.	PTP	Draw	PTP	Draw	PTP	Draw
ETL	0.84	0.82	0.52	0.53	0.49	0.49	0.41	0.42
PF	0.80	0.82	0.52	0.56	0.53	0.56	0.47	0.46

Table S4. Model Performance (RMSE) for the OCO-3 self crossing simulation. ETL and PF are the only sites shown due to the locations of OCO-3 self crossings. The column descriptions follow Table S1.

Site	Training		Testing		Opt. Extendibility		Pess. Extendibility	
	PTP	Draw.	PTP	Draw	PTP	Draw	PTP	Draw
ETL	0.15	0.21	0.30	0.43	0.27	0.40	0.31	0.36
PF	0.13	0.18	0.25	0.37	0.31	0.40	0.34	0.50

Table S5. Model Performance (R^2) for the OCO-2/3 growing season simulation. The column descriptions follow Table S1.

Site	Training		Testing		Opt. Extendibility		Pess. Extendibility	
	PTP	Draw.	PTP	Draw	PTP	Draw	PTP	Draw
ETL	0.85	0.84	0.56	0.52	0.50	0.53	0.42	0.40
PF	0.85	0.83	0.55	0.53	0.55	0.54	0.46	0.40
Lauder	0.86	0.85	0.54	0.52	0.54	0.53	0.43	0.40
Lamont	0.86	0.84	0.55	0.55	0.53	0.51	0.47	0.44

Table S6. Model Performance (RMSE) for the OCO-2/3 growing season simulation. The column descriptions follow Table S1.

Site	Training		Testing		Opt. Extendibility		Pess. Extendibility	
	PTP	Draw.	PTP	Draw	PTP	Draw	PTP	Draw
ETL	0.12	0.17	0.26	0.37	0.30	0.42	0.35	0.58
PF	0.12	0.17	0.25	0.35	0.32	0.44	0.35	0.57
Lauder	0.13	0.18	0.29	0.37	0.19	0.29	0.23	0.28
Lamont	0.12	0.17	0.25	0.36	0.30	0.39	0.34	0.48

Table S7. Model Performance (R^2) for the simulation where full diurnal cycles (27 quarter hour interval points) are given to the model as input data. The column descriptions follow Table S1, but there is no optimistic versus pessimistic version of the extendibility test, as there is no simulated error added to these simulations.

Site	Training		Testing		Extendibility	
	PTP	Draw.	PTP	Draw	PTP	Draw
ETL	0.96	0.97	0.92	0.91	0.90	0.90
PF	0.96	0.96	0.93	0.94	0.96	0.96
Lauder	0.95	0.96	0.94	0.95	0.94	0.95
Lamont	0.95	0.97	0.93	0.93	0.96	0.96

Table S8. Model Performance (RMSE) for the simulation where full diurnal cycles (27 quarter hour interval points) are given to the model as input data. The column descriptions follow Table S1, but there is no optimistic versus pessimistic version of the extendibility test, as there is no simulated error added to these simulations.

Site	Training		Testing		Extendibility	
	PTP	Draw.	PTP	Draw	PTP	Draw
ETL	0.06	0.08	0.09	0.13	0.11	0.13
PF	0.07	0.08	0.08	0.10	0.06	0.08
Lauder	0.07	0.09	0.07	0.09	0.08	0.11
Lamont	0.07	0.09	0.09	0.11	0.06	0.07